# Effects of ground-state correlations on muon capture matrix elements*

R. J. McCarthy† and G. E. Walker
*Department of Physics, Indiana University, Bloomington, Indiana 47401*
(Received 1 July 1974)

The muon capture matrix elements $M_v^2$, $M_a^2$, and $M_p^2$ are calculated for $^4$He and $^{16}$O using the closure approximation and utilizing the linked cluster expansion to introduce correlations in the nuclear target wave functions. An important set of diagrams is summed by replacing uncorrelated wave functions with Bethe-Goldstone wave functions. However, we also find it necessary to include diagrams insuring that the pair number operator is unchanged and (for $^{16}$O) particle-hole diagrams to account for the fact that oscillator orbitals rather than Hartree-Fock orbitals are used for the uncorrelated basis. Typical results for $^{16}$O are $M_v^{2(\mathrm{corr})} = 0.82 M_a^{2(\mathrm{corr})} = 0.74 M_p^{2(\mathrm{corr})} = 0.58 M^{2(\mathrm{osc})}$, while for $^4$He, $M_v^{2(\mathrm{corr})} = 0.88 M_a^{2(\mathrm{corr})} = 0.78 M_p^{2(\mathrm{corr})} = 0.76 M^{2(\mathrm{osc})}$. The bulk of the effects arise from correlations induced by the tensor component of the nucleon-nucleon interaction. We find that including correlations reduces the predicted total capture rate by $\sim 30\%$ in $^{16}$O and $\sim 20\%$ in $^4$He.

[NUCLEAR REACTIONS $^4$He, $^{16}$O, calculated total muon capture rate, closure and nuclear correlations.]

## I. INTRODUCTION

### A. Historical

In general, to make muon capture predictions for complex nuclei one must adopt several global assumptions regarding the muon-nucleon weak interaction coupling constants as well as utilizing some model for the nuclear target wave functions. Some early approaches to muon capture concentrated on testing the validity of the various assumptions adopted to relate the appropriate muon capture coupling constants to coupling constants appearing in other weak and electromagnetic processes. For example, Foldy and Walecka[1,2] and Primakoff and Kim[3] adopted standard assumptions regarding the $\mu$-capture coupling constants and related muon capture *matrix elements* to matrix elements appearing in other processes such as photoabsorption, $\beta$ decay, and electron scattering. Thus, the appropriate muon capture matrix element strength could be obtained from experimental data involving other processes without making detailed assumptions about nuclear wave functions. Using this approach, comparison of predictions with experiments to date confirms one's confidence in the validity of the standard assumptions for the muon capture coupling constants (although, apparently, the induced pseudoscalar coupling constant value has still not been strenuously tested).

If one has confidence in the form of the muon capture effective Hamiltonian and values of the coupling constants, then the capture process can be used to probe the nucleus, i.e., test proposed nuclear model wave functions. Historically, predictions of partial or total capture rates in light closed shell nuclei using the particle-hole (p-h) shell model have not been in good agreement with experimental results. For example, calculated *total* capture rates for $^{16}$O have overestimated the experimental result by roughly a factor of 1.5 to 2.[4,5] For the case of the *known* partial transitions in $^{16}$O leading to the lowest states in $^{16}$N, reduction factors are also frequently required. Subsequent investigation[6,7] has demonstrated that including (reasonably well motivated) two-particle two-hole admixtures in the ground states of "closed shell nuclei" can substantially improve the agreement with experiment for particular partial transitions (especially to low lying p-h final states of the daughter nucleus). However, the situation for the total capture rate has not yet been reconciled by adopting this particular configuration mixing mechanism.[8]

For practical purposes shell model calculations are usually performed in a greatly restricted basis using a nonsingular residual interaction. Thus as we test in more detail the nuclear wave functions obtained in this manner it is no surprise that they are found inadequate. In particular, the presence of a very strong short range repulsion (the "hard core") and a longer range noncentral spin dependent interaction (the tensor force) in the realistic nucleon-nucleon interaction makes it improbable that the model nuclear wave functions one traditionally uses (even for "closed shell" nuclei) are correct in detail (although to be sure the simple model wave functions can often yield the correct energy location and relative strength of various transition processes). This criticism of nuclear model wave functions to date is not limited to p-h calculations, but also applies

to calculations of the type given in Refs. 6, 7, and 8 where, for reasons of practicality, it was necessary to severely limit the type of nuclear configuration mixing studied.

Faced with the complexities of correctly describing a strongly interacting many-body system, Migdal[9] has recast the problem so that effects apparently very difficult to calculate from first principles (i.e., starting with a realistic nucleon-nucleon interaction and actually evaluating the appropriate series of diagrams in the many-body environment) become parametrized as renormalization constants multiplying various nucleon spin, isospin, and momentum operators that often appear in single particle transition matrix elements. By employing appropriate experimental data the renormalization constants may be determined and then used in making predictions regarding other processes. When applied to muon capture,[10] the Migdal theory is not entirely satisfying since: (1) one has little or no evidence concerning the validity of the several simplifying assumptions that must be adopted, and relatedly, (2) the underlying "microscopic" reason for the operator renormalization remains hidden. The latter point is particularly distressing if our goal is a better understanding of nuclear many-body systems as opposed to simply relating muon capture to other processes.

### B. Present work

The motivation for the present work is to understand the effect of correlations on total muon capture rates in terms of a more microscopic theory. This necessitates the use of a realistic nucleon-nucleon interaction to obtain the correlated wave functions to be used in the formalism. Techniques exist for incorporating realistic correlations in the nuclear many-body wave function and in this paper we shall employ these techniques to study the effect of correlations on total muon capture rates in the closure approximation. It is realized that in order for our results to be useful in increasing the understanding of the effects of correlations, particular attention must be paid to several technical aspects associated with adopting the linked cluster expansion and the Bethe-Goldstone (BG) equation which is used to obtain the correlated nuclear wave functions. We shall not be primarily interested in obtaining detailed fits to experimental total capture rates. Instead we focus our attention on the *ratio* of muon capture matrix elements obtained using correlated wave functions (for a given average neutrino energy) to capture matrix elements obtained using the usual shell model wave functions (assuming the same average neutrino energy). Considerable emphasis in this study is given to the effects on the predicted capture rates of the intermediate state spectrum and the Pauli operator adopted in solving the BG equation. We also discuss the corrections required due to the fact that Hartree-Fock single particle wave functions have not been used as the elementary uncorrelated basis functions.

In the next section we list the formulas needed for our discussion of the capture process. In particular, formulas required to calculate various muon capture matrix elements in the closure approximation are given.

In Sec. III we present the techniques used to introduce correlations in the nuclear wave functions and describe the calculation of the BG wave function. Our results for calculations on $^4$He and $^{16}$O are presented and discussed in Sec. IV. The author's assessments of the limitations of the calculation presented in this paper and suggestions for further investigations are included at the end of Sec. IV.

## II. MUON CAPTURE MATRIX ELEMENTS

The basic process under consideration is the absorption of a negative $\mu$ meson from an atomic orbit on a proton in the nucleus resulting in the creation of a neutron and a neutrino, i.e.,

$$\mu^- + N(A, Z) \rightarrow N^*(A, Z-1) + \nu \ , \tag{1}$$

where $N^*$ represents a state of the daughter nucleus. The formula for calculating the total muon capture rate $\Lambda_{\mu c}$ on a complex nucleus may be written in the form

$$\Lambda_{\mu c} = \nu_\mu{}^2 \frac{(|\varphi_\mu|^2)_{\text{ave}}}{2\pi\hbar^2 c} \times [G_v{}^2 M_v{}^2 + 3G_a{}^2 M_a{}^2 + (G_p{}^2 - 2G_p G_a) M_p{}^2] + \Lambda'_{\mu c} \ . \tag{2}$$

In Eq. (2) the symbol $\Lambda'_{\mu c}$ represents recoil corrections to the capture rate (~10% in $^{16}$O),[1] $G_v$, $G_p$, and $G_a$ are "effective" coupling constants, and $(|\varphi|^2)_{\text{ave}}$ is the square of the muon atomic wave function averaged over the nucleus. The muon capture nuclear matrix elements $M_v{}^2$, $M_a{}^2$, and $M_p{}^2$ are defined by

$$M^2 \equiv \bar{\sum_a} \sum_b \left(\frac{\nu_{ab}}{\nu_\mu}\right)^2 \times \int \frac{d\hat{\vec{\nu}}}{4\pi} \left| \left\langle b \left| \sum_{i=1}^{A} \tau_i^{(-)} O(i) e^{-i\vec{\nu}_{ab} \cdot \vec{x}(i)} \right| a \right\rangle \right|^2 , \tag{3}$$

where for

$$M_v^2, \quad O(i) \equiv 1 \ ;$$

$$M_a^2, \quad O(i) \equiv \vec{\sigma}_i/\sqrt{3} \ ; \tag{4}$$

$$M_p^2, \quad O(i) \equiv \hat{\vec{\nu}} \cdot \vec{\sigma}_i \left( \hat{\vec{\nu}} \equiv \frac{\vec{\nu}_{ab}}{|\nu_{ab}|} \right) ;$$

and the muon rest mass energy $\hbar\nu_\mu c \equiv m_\mu c^2$ is related to the neutrino energy $\hbar\nu_{ab}c$ via

$$m_\mu c^2 = \hbar\nu_{ab}c + E_b - E_a + (\text{small atomic, nuclear Coulomb, and } n\text{-}p \text{ mass difference effects}) . \tag{5}$$

The kets $|a\rangle$ and $|b\rangle$ denote, respectively, the initial and final nuclear many-body states.

We shall concentrate on the evaluation of the matrix elements $M_v^2$, $M_p^2$, and $M_a^2$ using the closure approximation, since our primary interest is the effect of correlations on the *total* capture rate. The matrix elements under consideration may be written in the form ($J_a = 0$ assumed hereafter)

$$\sum_b f(\nu_{ab}) \left\langle a \left| \sum_{j=1}^{A} O_j^\dagger(\nu_{ab}) \right| b \right\rangle \left\langle b \left| \sum_{i=1}^{A} O_i(\nu_{ab}) \right| a \right\rangle . \tag{6}$$

If the capture process is associated primarily with excitation of nuclear states concentrated in an appropriately narrow energy region (depending on the variation of $f(\nu_{ab})$ and $\langle b|O(\nu_{ab})|a\rangle$ with $E_b$) then one can ignore the final state dependence in $f(\nu_{ab})$ and $O(\nu_{ab})$ and use closure on the states $|b\rangle$:

$$\sum |b\rangle\langle b| = 1 , \tag{7}$$

to reduce Eq. (6) to the form

$$f(\bar{\nu}) \left\langle a \left| \sum_{i,j=1}^{A} O_j^\dagger(\bar{\nu}) O_i(\bar{\nu}) \right| a \right\rangle . \tag{8}$$

The "average" neutrino momentum $\bar{\nu}$ appearing in Eq. (8) should be determined from Eq. (5) by inserting for $E_b$ a representative value of the "narrow" band of energies where the strength is concentrated. Of course one can also treat $\bar{\nu}$ as an adjustable parameter, in which case one would be able to guarantee a fit to the total capture rates. Our approach is to adopt a value of $\bar{\nu}$ consistent with previous studies of partial transition rates and then to see how, for this fixed value of $\bar{\nu}$, correlations in the ground state wave function alter the predicted total capture rate. Earlier investigations on closed shell nuclei either based on Wigner super-multiplet theory[1] or using the results of particle-hole shell model calculations,[5,11] have predicted that over 90% of the muon capture strength should be associated with final nuclear states $|b\rangle$ located in the giant dipole resonance region (for $^{16}$O this implies analog states of excitation energy ~23 MeV ± 3 MeV). Actually adopting values of $\bar{\nu}$ consistent with assuming the capture strength is concentrated in the giant resonance region leads, for capture on $^{16}$O, to a predicted capture rate 1.5 to 2 times greater than experimentally observed [if a simple closed shell model $4(1s)+12(1p)$ ground state is adopted].[4] Similar overestimates result if one simply sums the partial transition rates obtained from assuming a closed shell ground state and using a particle-hole model (with residual interaction diagonalization) for the final nuclear states.

In what follows we list more explicit formulas for evaluating expression (8). It is convenient to separate the sum over $i$ and $j$ in Eq. (8) into two parts: $i=j$ and $i\neq j$. The sum $i=j$ (which yields a one-body operator that is a projection operator for protons) is easily carried out for the muon capture operators, yielding

$$\left(\frac{\bar{\nu}}{\nu_{ab}}\right)^2 Z \text{ for } M_v^2, \ M_a^2, \text{ and } M_p^2 . \tag{9}$$

For $i\neq j$ the actual two-body matrix elements that must be evaluated are of the form

$$2\left(\frac{\bar{\nu}}{\nu_{ab}}\right)^2 \sum_{AB} \langle n_A l_A l_{ZA} t_{ZA} s_{ZA}, n_B l_B l_{ZB} t_{ZB} s_{ZB} | \tau_1^{(+)} \tau_2^{(-)} e^{-i\vec{\nu}\cdot(\vec{x}_2 - \vec{x}_1)} O_{12} | n_A l_A l_{ZA} t_{ZA} s_{ZA}, n_B l_B l_{ZB} t_{ZB} s_{ZB} \rangle_{\text{anti}} , \tag{10}$$

where for

$$M_v^2, \quad O_{12} \equiv 1 \ ;$$

$$M_p^2, \quad O_{12} \equiv \hat{\vec{\nu}} \cdot \vec{\sigma}_1 \hat{\vec{\nu}} \cdot \vec{\sigma}_2 \ ;$$

$$M_a^2, \quad O_{12} = \tfrac{1}{3}\vec{\sigma}_1 \cdot \vec{\sigma}_2 .$$

In Eq. (10) we have assumed, for definiteness, a single particle shell model for the target nucleons. The sum over $A$ and $B$ is over levels occupied in the ground state. The factor of 2 appearing in Eq. (10) would not normally be present if one takes the expectation value of a two-body operator such as the mutual interaction energy $\sum_{i<j} V_{ij}$, but is present here because the restriction $i<j$ is not present

in Eq. (8). Assuming a closed shell ground state and adopting harmonic oscillator single particle orbitals, one can easily evaluate Eq. (10). Combining the results with Eq. (9) for $i=j$ yields $(M_v{}^2 = M_p{}^2 = M_a{}^2)$ for $^4$He $(1s^4)$

$$M_v{}^2 = \left(\frac{\bar{\nu}}{\nu_\mu}\right)^2 (2 - 2e^{-2y}) \ , \tag{11a}$$

while for $^{16}$O$(1s^4, 1p^{12})$

$$M_v{}^2 = \left(\frac{\bar{\nu}}{\nu_\mu}\right)^2 [8 - 8e^{-2y}(1+y^2)] \ . \tag{11b}$$

Here $y = (\frac{1}{2}\bar{\nu}b)^2$ and $b = (\hbar/M_p\omega)^{1/2}$ is the usual oscillator constant. Equations (11a) and (11b) yield what we shall refer to as the muon capture matrix elements in the closure approximation using uncorrelated wave functions.

We wish to transform expression (10) to a form where one may replace the simple shell model wave functions by correlated wave functions obtained from solving the BG equation. It is therefore useful to rewrite Eq. (10) in a form where the wave function depending on the relative coordinate $\vec{r} = \vec{x}_2 - \vec{x}_1$ appears explicitly. We obtain

$$\sum_{AB} \langle n_A l_A l_{ZA} t_{ZA} s_{ZA} n_B l_B l_{ZB} t_{ZB} s_{ZB} | \tau_1^{(+)} \tau_2^{(-)} [O^\lambda(\vec{r}) \times O^\lambda(\vec{\sigma})]_0^0 | n_A l_A l_{ZA} t_{ZA} s_{ZA} n_B l_B l_{ZB} t_{ZB} s_{ZB} \rangle_{\text{anti}}$$

$$= - \sum_{\substack{n_A l_A \\ n_B l_B \\ nl N\mathfrak{L} \\ SL\mathfrak{J}T}} [(-1)^T] \frac{(2L+1)(2\mathfrak{J}+1)^{1/2}}{(2l+1)} |\langle nlN\mathfrak{L}, L | n_A l_A n_B l_B, L\rangle|^2 (nlS\mathfrak{J} \| [O^\lambda(\vec{r}) \times O^\lambda(\vec{\sigma})]^0 \| nlS\mathfrak{J})_{\text{anti}} \ , \tag{12}$$

where the bracketed expression $\langle nlN\mathfrak{L}, L | n_A l_A n_B l_B, L\rangle$ is a standard Moshinsky bracket. Since we are considering only $J=0$ nuclei, the rank of the operator appearing in Eq. (12), i.e., $[O^\lambda \times O^{\lambda'}]^k$, must have $k=0$. The particular form for the operator appearing in Eq. (12) depends on whether one is evaluating $M_v{}^2$, $M_a{}^2$, or $M_p{}^2$.

For $M_v{}^2$

$$e^{i\vec{\bar{\nu}}\cdot\vec{r}} = \sum_\lambda i^\lambda \{(2\lambda+1)4\pi\}^{1/2} j_\lambda(\bar{\nu}r) Y_{\lambda 0}(\Omega_{\vec{r}}), \quad k=0 \to \lambda = 0 \ ,$$

and (13a)

$$O^\lambda(\vec{r}) = (4\pi)^{1/2} j_0(\bar{\nu}r) Y_0(\Omega_{\vec{r}}), \quad O^\lambda(\vec{\sigma}) = 1 \ .$$

For $M_a{}^2$

$$\tfrac{1}{3} e^{i\vec{\bar{\nu}}\cdot\vec{r}} \vec{\sigma}_1 \cdot \vec{\sigma}_2 = \sum_\lambda i^\lambda \{(2\lambda+1)4\pi\}^{1/2} j_\lambda(\bar{\nu}r) Y_{\lambda 0}(\Omega_{\vec{r}}) [(-\sqrt{3}/3 \ [\sigma_1 \times \sigma_2]^0], \quad k=0 \to \lambda = 0 \ ,$$

and (13b)

$$O^\lambda(r) = (4\pi)^{1/2} j_0(\bar{\nu}r) Y_0(\Omega_{\vec{r}}), \quad O^\lambda(\vec{\sigma}) = (-1/\sqrt{3}) [\vec{\sigma}_1 \times \vec{\sigma}_2]^0 \ .$$

For $M_p{}^2$

$$e^{i\vec{\bar{\nu}}\cdot\vec{r}} \sigma_{1z}\sigma_{2z} = \sum_\lambda i^\lambda \{(2\lambda+1)4\pi\}^{1/2} j_\lambda(\bar{\nu}r) Y_{\lambda 0}(\Omega_{\vec{r}}) \{-(1/\sqrt{3})[\sigma_1 \times \sigma_2]^0 + (\tfrac{2}{3})^{1/2} [\sigma_1 \times \sigma_2]_0^2\} \ , \tag{13c}$$

$$k=0 \to \lambda = 2, 0.$$

For $\lambda = 0$

$$O^0(\vec{r}) = (4\pi)^{1/2} j_0(\bar{\nu}r) Y_0(\Omega_{\vec{r}}) \ ,$$

$$O^0(\vec{\sigma}) = -\frac{1}{\sqrt{3}} [\vec{\sigma}_1 \times \vec{\sigma}_2]^0 \ . \tag{13d}$$

For $\lambda = 2$

$$[O^2(\vec{r}) \times O^2(\vec{\sigma})]^0 = -(8\pi/3)^{1/2} j_2(\bar{\nu}r) Y_2(\Omega_{\vec{r}}) [\vec{\sigma}_1 \times \vec{\sigma}_2]^2 \ . \tag{13e}$$

It is important to note that for correlated wave functions the matrix element $(nlS\mathfrak{J} \| O \| nlS\mathfrak{J})$ will be a function of $\vec{\mathfrak{J}} = \vec{l} + \vec{S}$ so the sum over $\mathfrak{J}$ in expression (12) cannot be trivially performed. In the simple single particle (uncorrelated) picture the contribution of the operator given by expression (13e) for $M_p{}^2$ vanishes and one immediately obtains $M_p{}^2 = M_a{}^2$.

## III. CORRELATIONS AND THE BETHE-GOLDSTONE WAVE FUNCTION

### A. Linked cluster expansion

To obtain the simple results in the preceding section we assumed that the ground state wave function was a Slater determinant of single particle (SP) harmonic oscillator (HO) wave functions. The ground state expectation value of a sum of two-body operators could then be written as a simple sum over (relative) two-body matrix elements. We now want to extend our calculations to allow for the existence of 1p-1h and 2p-2h correlations in the ground state wave function. Our approach is based on the linked cluster formalism for calculating ground state expectation values.[12] The expectation value of a two-body operator is given as a sum of Brueckner-Goldstone diagrams.

The diagrams shown in Fig. 1 can be summed by replacing matrix elements of the operator between uncorrelated two-body wave functions by matrix elements calculated between correlated (BG) wave functions. That is,

$$\langle \Phi_{AB} | O_{12} | \Phi_{AB} \rangle \rightarrow \langle \Psi_{AB} | O_{12} | \Psi_{AB} \rangle \ , \tag{14}$$

where $\Psi_{AB}$ is defined in the SP basis by

$$\Psi_{AB}(\omega_{AB}) = \Phi_{AB} + \sum_{ab} \frac{Q_{ab} G_{AB,ab} \Phi_{ab}}{\omega_{AB} - E_a - E_b} \ . \tag{15}$$

Here $\Phi$ is a two particle HO wave function; $Q_{ab}$ projects into unoccupied SP states ($Q_{ab}=0$ if $a$ *or* $b$ is occupied); $\omega_{AB}=E_A+E_B$ is the starting energy of the two nucleons interacting; $E_a+E_b$ is the energy of the intermediate (unoccupied) two particle state; and $G$ is the nuclear reaction matrix.

It is possible to include a selected class of higher order diagrams by normalizing the BG wave functions. The lowest order (in $G$) diagrams of this class are shown in Fig. 2. These diagrams are needed to ensure correct normalization of the number of pairs[13] in the nucleus and will turn out to have an important effect on our results.

The diagrams shown in Fig. 3 are the lowest order diagrams needed to account for the fact that our unperturbed ground state is a Slater determinant composed of HO SP wave functions rather than SP wave functions determined through a Hartree-Fock procedure. These 1p-1h diagrams cannot be included by modifying the correlated two-body wave function and must be calculated separately. Thus in our results we will refer to the 2p-2h contributions as those which are obtained by the replacement

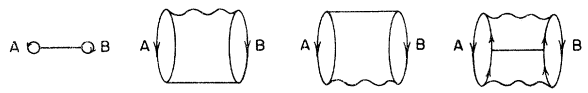


FIG. 1. Linked cluster diagrams summed by replacing uncorrelated wave functions with conventionally normalized BG wave functions. The solid lines represent muon capture operators, while wiggly lines represent $G$ matrix interactions.

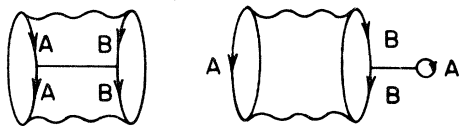


FIG. 2. Lowest order diagrams included by renormalizing the BG wave functions.

$$\langle \Phi_{AB} | O | \Phi_{AB} \rangle \rightarrow \frac{\langle \Psi_{AB} | O | \Psi_{AB} \rangle}{\langle \Psi_{AB} | \Psi_{AB} \rangle} \ , \tag{16}$$

and the 1p-1h contributions as those which are obtained by directly evaluating the diagrams in Fig. 3. The latter contribution turns out to be of some importance for $^{16}$O but not for $^{4}$He.

### B. Calculation of the Bethe-Goldstone wave function

Two problems arise in trying to evaluate the BG wave function from Eq. (15). The first problem is that the unoccupied SP state energies $E_a$ and $E_b$ are not unique. We have chosen our basis states to be defined by HO wave functions. However, we are free to define the zero of our HO potential in any way we like in an attempt to improve the convergence of the linked cluster expansion. Thus we will define the single particle energies by

$$E_\alpha = E_\alpha^{\rm osc} - C = (2n_\alpha + l_\alpha - \tfrac{1}{2})\hbar\omega - C \ , \tag{17}$$

where $C$ is an arbitrary parameter.

It is important to understand the relation between the constant $C$, the starting energy $\omega_{AB}$, and the energy gap between occupied and unoccupied states. For example, the $1p$ nucleons in $^{16}$O are bound by ~10 MeV so $\omega_{AB}=E_A+E_B \approx -20$ MeV for $|AB\rangle = |(1p)^2\rangle$. If we choose $C=0$, the energy needed to scatter both nucleons into the $2s$-$1d$ shell is given by $7\hbar\omega - (-20\ \text{MeV}) = 110$ MeV for

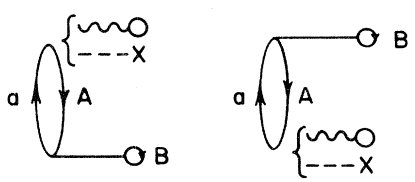


FIG. 3. Hartree-Fock contributions to the capture rate. The operator---×represents $(-U^{\rm osc})$.

$\hbar\omega = 12.8$ MeV. If we choose $C = 3\hbar\omega$ (a value which yields reasonable binding energies in Brueckner calculations[14,15]), the energy needed for a 2p-2h excitation into the $2s$-$1d$ shell is reduced to ~30 MeV, a value much closer to the usual shell model choice of $2\hbar\omega$. A similar argument for $^4$He favors a choice of $C \approx 2\hbar\omega$.

We do not attempt to specify an exact value of $C$ since we are not treating the occupied state energies exactly (e.g., we neglect spin-orbit splitting and Coulomb effects), and there are still a number of uncertainties in binding energy calculations about the "best" choice of intermediate state spectrum. Thus we will present our results for a number of values of $C$. However, we do wish to emphasize that the choice of $C \approx 2\hbar\omega$ for $^4$He and $3\hbar\omega$ for $^{16}$O is clearly consistent with our present understanding of nuclear many-body calculations.

The second difficulty in evaluating Eq. (15) for the BG wave function is purely technical in nature. The sum over unoccupied states extends to very high energies due to the strong short-range nature of realsitic nucleon-nucleon interactions. Thus it becomes much more convenient to work with an approximate BG wave function which is defined to separate in relative and center-of-mass (RCM) coordinates and to be diagonal in center-of-mass HO states. This approximation has been used quite extensively in binding energy calculations and shown to be satisfactory.[15] However, as we will discuss in detail later, muon capture cross sections are more sensitive to fine details of the calculation than are total binding energies. Thus the approximations we now make to transform into RCM coordinates are probably the most serious problem with our calculations. We will return to this question when discussing our results.

Since our basis states and intermediate state Hamiltonian already separate into RCM coordinates and are diagonal in center-of-mass HO states, the desired transformation to RCM coordinates can be carried out if we replace the exact Pauli operator $Q$ by an approximate Pauli operator. There are two common approximations for $Q$ which could be used. The first is the Eden-Emery[16] Pauli operator $Q_{\rm EE}$ which replaces the sum in Eq. (15) by a sum over all two particle states with energy greater than some chosen energy. For example, $Q_{\rm EE}(\mathfrak{N})$ excludes all two particle states with $2n_1 + l_1 + 2n_2 + l_2 = 2n + l + 2N + L \leq \mathfrak{N}$. The major advantage of using $Q_{\rm EE}$, aside from its obvious truncation advantages, is that $Q_{\rm EE}$ is diagonal in both the RCM and SP representations. The Eden-Emery $Q$ has a major problem, however, in that it cannot distinguish between 1p-1h and 2p-2h excitations and thus one cannot treat the intermediate state energies correctly.[15]

The second approximation for $Q$ is slightly more difficult to use but it does treat the difference between 1p-1h and 2p-2h excitations correctly on the average. We use Wong's[17] $GA(0)$ approximation for $Q$ in which matrix elements of $Q$ between RCM states no longer have the values 0 or 1 but are given by the overlap of the particular RCM states with allowed 2p-2h states. The matrix elements of $Q$ are averaged over the allowed total relative angular momentum for a given relative $l$, and matrix elements off-diagonal in center-of-mass states are ignored. With this choice for $Q$, which is commonly referred to as an angle-averaged $Q$ or $Q_{\rm AA}$, the energy denominators can be treated correctly and one can distinguish between 1p-1h and 2p-2h excitations. We will present results obtained with both approximations in order to show the sensitivity of our results to the Pauli operator. However, it is the results obtained using $Q_{\rm AA}$ that we consider more reliable.

With the above approximation on the Pauli operator $Q$ we can now define a relative BG wave function as

$$\Psi_{AB}(nlS\mathcal{J}NL;\omega_r) = \varphi_{nlS\mathcal{J}} + \sum_{n'l'} \frac{Q(n'l'NL)}{\omega_r - E^{\rm osc}_{n'l'}} G^{S\mathcal{J}NL}_{nl,n'l'}(\omega_r) \times \varphi_{n'l'S\mathcal{J}}, \quad (18)$$

where

$$\omega_r = E_A + E_B - E^{\rm osc}_{NL} + 2C \ . \quad (19)$$

The relative BG wave functions are obtained using the Barrett, Hewitt, and McCarthy (BHM) method,[18] adapted to calculations in the relative coordinate system. For relative $S$ states we included intermediate states up to $n' = 36$, while for higher partial waves $n' = 24$ was sufficient. The Pauli operator was set equal to 1 for $n' \geq 6$, which should cause no appreciable error. Note that for tensor coupled partial waves, where $l' = l$ and $2\mathcal{J} - l$, up to 72 HO states are included in the BG wave function.

When relative HO wave functions are replaced by BG wave functions, a number of complications are introduced into the formalism of Sec. II. In general, since the radial matrix elements now depend on relative $\mathcal{J}$, $M_a{}^2$ and $M_p{}^2$ are no longer equal to $M_v{}^2$. Moreover, since the total spin $S$ of the nucleus is no longer zero, $M_p{}^2$ is not equal to $M_a{}^2$.

For HO wave functions we have

$$\varphi^S_{nl}(\vec{r},\vec{\sigma}) = (1/r)R_{nl}(r)Y_{\mathcal{J}Sl}(\vec{\sigma},\Omega_{\vec{r}}) \ , \quad (20)$$

where $R_{nl}$ is the radial HO wave function and

$$Y_{\mathcal{J}Sl}(\sigma,\Omega_{\vec{r}}) = \sum_{m_S m_l} (lS; m_l m_S | \mathcal{J}M_{\mathcal{J}}) Y^{m_l}_l X^{m_S}_S \ . \quad (21)$$

In this case the right-hand side of Eq. (12) can be written as

$$\sum_{\substack{n_A l_A \\ n_B l_B \\ nlN\mathfrak{L} \\ STL\mathfrak{J} \\ (l+S+T \text{ odd})}} \frac{(-1)^{\mathfrak{J}+\lambda}}{(2\lambda+1)^{1/2}} \frac{(2L+1)(2\mathfrak{J}+1)}{(2l+1)} |\langle nlN\mathfrak{L}, L | n_A l_A n_B l_B, L\rangle|^2 \begin{Bmatrix} l & S & \mathfrak{J} \\ S & l & \lambda \end{Bmatrix} (S\| O^\lambda(\vec{\sigma})\| S)(nl\| O^\lambda(\vec{r})\| nl) \ . \tag{22}$$

Because the sum over $\mathfrak{J}$ can be easily performed, considerable further simplification is possible. However, for the case of correlated wave functions we obtain

$$\Psi^{\mathfrak{J}S}_{nll'}(\vec{r}, \vec{\sigma}) = (1/r)[u_l(r) Y_{\mathfrak{J}Sl}(\vec{\sigma}, \Omega_r^{\rightarrow}) + w_{l'}(r) Y_{\mathfrak{J}Sl'}(\vec{\sigma}, \Omega_r^{\rightarrow})] \tag{23}$$

$$l' = l \pm 2 \text{ if } \mathfrak{J} = l \pm 1 \ ,$$

and the right-hand side of Eq. (12) becomes

$$\sum_{\substack{n_A l_A \\ n_B l_B \\ nlN\mathfrak{L} \\ STL\mathfrak{J} \\ (l+S+T \text{ odd})}} \frac{(-1)^{\mathfrak{J}+\lambda}(2L+1)(2\mathfrak{J}+1)}{(2l+1)(2\lambda+1)^{1/2}} |\langle nlN\mathfrak{L}, L | n_A l_A n_B l_B, L\rangle|^2 (S\| O^\lambda(\vec{\sigma})\| S$$

$$\times \left[ \begin{Bmatrix} l & S & \mathfrak{J} \\ S & l & \lambda \end{Bmatrix} (nl\| O^\lambda(\vec{r})\| nl) + 2 \begin{Bmatrix} l & S & \mathfrak{J} \\ S & l' & \lambda \end{Bmatrix} (nl\| O^\lambda(\vec{r})\| nl') + \begin{Bmatrix} l' & S & \mathfrak{J} \\ S & l' & \lambda \end{Bmatrix} (nl'\| O^\lambda(\vec{r})\| nl') \right] \ . \tag{24}$$

Since the $u$'s and $w$'s depend on $\mathfrak{J}$, further simplification is not possible. We have employed Eq. (24) to calculate muon capture matrix elements using correlated wave functions.

Finally, we list the expression needed to evaluate the 1p-1h diagrams shown in Fig. 3. We have

$$\Delta M^2(\text{1p-1h}) = -\sum_{n_a n_A l_A} \frac{1}{4(2l_A+1)} \Bigg\{ \sum_{\substack{L'S'T' \\ \underline{n}'\underline{n}l n_B \\ \underline{\mathfrak{N}}\underline{\mathfrak{L}} l_B}} (-1)^{T'}(2L'+1)(2S'+1)[1-(-1)^{\underline{l}+S'+T'}]$$

$$\times \langle \underline{n}'\underline{l}\underline{\mathfrak{N}}\underline{\mathfrak{L}}, L' | n_a l_a n_B l_B, L'\rangle \langle \underline{n}l\underline{\mathfrak{N}}\underline{\mathfrak{L}}, L' | n_A l_A n_B l_B, L'\rangle \langle \underline{n}'\underline{l}| j_0(\overline{\nu}r)|\underline{n}l\rangle \Bigg\}$$

$$\times \frac{1}{E_{n_A l_A} - E_{n_a l_a}} \Bigg[ \sum_{\substack{n_C l_C \\ LS\mathfrak{J}T}} (2T+1)(2L+1)(2\mathfrak{J}+1) \sum_{\substack{nn'l \\ \mathfrak{N}\mathfrak{L}}} \frac{1}{(2l+1)}$$

$$\times \langle n'l\mathfrak{N}\mathfrak{L}, L | n_a l_A n_C l_C, L\rangle \langle nl\mathfrak{N}\mathfrak{L}, L | n_A l_A n_C l_C, L\rangle$$

$$\times \langle n'l\mathfrak{N}\mathfrak{L}S\mathfrak{J}T | G | nl\mathfrak{N}\mathfrak{L}S\mathfrak{J}T\rangle_{\text{anti}} - 4(2l_A+1)\langle n_a l_A | U^{\text{osc}} | n_A l_A\rangle \Bigg] . \tag{25}$$

## IV. RESULTS AND CONCLUSIONS

### A. Results

All of the results presented are calculated using the Hamada-Johnston nucleon-nucleon potential and bound state SP energies:

$$E_{1s} = -20 \text{ MeV for } {}^4\text{He} \ ,$$

and

$$E_{1s} = -30 \text{ MeV}, \quad E_{1p} = -10 \text{ MeV for } {}^{16}\text{O} \ .$$

Coulomb effects and spin-orbit splitting have been neglected because of the large uncertainty in unoccupied state SP energies.

We would first like to demonstrate the sensitivity of our results to various parameters and approximations used in the calculations. Thus in Table I we show the reduction factor

$$R = [M_v{}^2(\text{osc}) - M_v{}^2(\text{BG})]/M_v{}^2(\text{osc}) \tag{26}$$

obtained for $^{16}$O using various values of the energy parameter $C$ and a number of approximations on the Pauli operator. The results presented in Table I were obtained using an oscillator parameter $\hbar\omega = 12.8$ MeV and average neutrino momentum $\overline{\nu} = 0.5$ fm$^{-1}$. It turns out that the reduction factors for $M_v{}^2$, $M_a{}^2$, and $M_p{}^2$ (but, of course, not the total capture rate) are roughly independent of both $\overline{\nu}$ and $\hbar\omega$.

TABLE I. Reduction factor in $M_v^2$ obtained for $^{16}O$ using various values of $C$ and different approximations to the Pauli operator. $\hbar\omega = 12.8$ MeV, $\bar{\nu} = 0.5$ fm$^{-1}$.

| $C$ (MeV) | $Q_{EE}$ (6) (%) | $Q_{EE}$ (7) (%) | $Q_{EE}$ (8) (%) | $Q_{AA}$ (%) |
|---|---|---|---|---|
| 0 | 21 | 16 | 9 | 10 |
| 20 | 43 | 31 | 13 | 15 |
| 30 | 68 | 48 | 20 | 21 |
| 38.4 | | | 29 | 31 |

We should first point out that $Q_{EE}(6)$ and $Q_{EE}(7)$ are not good approximations to $Q$ for $^{16}O$. We have included these results only to show the extreme sensitivity of our calculations to the treatment of the Pauli operator. This sensitivity of $R$ to both $Q$ and the energy parameter $C$ indicates that the important correlations are relatively long ranged and tend to populate low-lying 2p-2h states.

If the normalization diagrams were not included in the calculation, the results for different approximations on $Q$ would show even more discrepancy. From Eq. (15) we see that

$$\langle \Psi_{AB} | \Psi_{AB} \rangle = \langle \Phi_{AB} | \Phi_{AB} \rangle + 2 \left\langle \Phi_{AB} \left| \frac{Q}{e} G \right| \Phi_{AB} \right\rangle + \left\langle \Phi_{AB} \left| G \frac{Q}{e} \frac{Q}{e} G \right| \Phi_{AB} \right\rangle \ . \quad (27)$$

If $Q$ is treated exactly (which is not possible in the RCM representation) the second term on the right-hand side of Eq. (27) vanishes. However, various approximations for $Q$ yield substantially different normalization effects. If we ignored the normalization we would be making successively larger errors going from $Q_{AA}$ and $Q_{EE}(8)$ down to $Q_{EE}(6)$. If calculations were carried out neglecting altogether both $Q$ and the normalization, the results could be off by orders of magnitude.

In Table II we present our main results for $^{16}O$ and $^4He$. Again, our results are presented in terms of reduction factors for the three matrix elements $M_v^2$, $M_a^2$, and $M_p^2$. In each case we show $R_1(M^2)$ which is the reduction factor obtained when 2p-2h correlations are taken into account and $R_T(M^2)$ which also includes the contribution of 1p-1h diagrams. Note that the reduction factors are roughly independent of $\bar{\nu}$ and $\hbar\omega$ and are substantially larger for $^{16}O$ than for $^4He$. It can also be seen that the 1p-1h diagrams of Fig. 3 have negligible contribution for $^4He$ but are appreciable for $^{16}O$.

The results of Table II are presented using what we consider "reasonable" values for the energy parameter $C$. Note, however, that the excitation energy involved in a 2p-2h excitation is still larger than that used in shell model calculations. Thus it would not be surprising if a more detailed calculation were able to obtain larger reduction factors than are presented here.

Why is it that two-body correlations seem to produce such large effects in muon capture matrix elements when the momentum transfers involved are relatively small? It is obvious from Table II that the value of the momentum transfer is not important. It is clear how these effects arise if one looks at the expression for the $M_v^2$ matrix element of $^4He$. Aside from multiplicative factors we have

$$M_v^2(\text{osc}) = 2 - 2\langle R_{1s}(r) | j_0(\bar{\nu}r) | R_{1s}(r) \rangle \ ,$$

while for correlated wave functions we have

$$M_v^2 = 2 - [3\langle \Psi(^3S_1) | j_0(\bar{\nu}r) | \Psi(^3S_1) \rangle / \langle \Psi(^3S_1) | \Psi(^3S_1) \rangle] + [\langle \Psi(^1S_0) | j_0(\bar{\nu}r) | \Psi(^1S_0) \rangle / \langle \Psi(^1S_0) | \Psi(^1S_0) \rangle] \ . \quad (28)$$

For $\hbar\omega = 21.75$, $\bar{\nu} = 0.4$ fm$^{-1}$, $C = 2\hbar\omega$ we find

$$M_v^2(\text{osc}) = 2 - 2\ (0.8586) = 0.2829$$

and

$$M_v^2 = 2 - [3(0.9973)/1.127] + [(0.8918)/1.024] = 0.2160$$

Thus, while individual (normalized) matrix elements of $j_0$ change by only 2 or 3%, $M_v^2$ changes by ~24% due to cancellations among terms of roughly

TABLE II. Reduction factors for $M_v^2$, $M_a^2$, and $M_p^2$ calculated without ($R_1$) and with ($R_T$) the 1p-1h contribution. The results were obtained using $Q_{AA}$.

| Nucleus | $\hbar\omega$ | $C$ | $\bar{\nu}$ | $R_1(M_v^2)$ (%) | $R_T(M_v^2)$ (%) | $R_1(M_a^2)$ (%) | $R_T(M_a^2)$ (%) | $R_1(M_p^2)$ (%) | $R_T(M_p^2)$ (%) |
|---|---|---|---|---|---|---|---|---|---|
| $^{16}O$ | 12.8 | $3\hbar\omega$ | 0.5 | 31 | 42 | 18 | 29 | 10 | 21 |
| | 14.0 | $3\hbar\omega$ | 0.5 | 30 | 41 | 19 | 30 | 11 | 21 |
| | 14.0 | $3\hbar\omega$ | 0.3 | 30 | 42 | 15 | 28 | 9 | 21 |
| $^4He$ | 21.75 | $2\hbar\omega$ | 0.3 | 24 | 24 | 14 | 14 | 2 | 2 |
| | 21.75 | $2\hbar\omega$ | 0.4 | 24 | 24 | 14 | 14 | 2 | 2 |

equal magnitude. It is also obvious that the correlations are much stronger in the tensor coupled $^3S_1$ state than in the $^1S_0$ state.

The $M_v{}^2$ matrix element of $^4$He is also useful in examining the effects of normalization. If we neglected to normalize the BG wave function we would obtain

$$M_v{}^2 \text{ (unnormalized)} = 2 - 3(0.9973) + (0.8918)$$
$$= -0.10 ,$$

a negative muon capture rate. Finally, we can determine whether the bulk of the normalization effect is obtained by calculating the diagrams of Fig. 2, or if higher order diagrams are also important.

Consider the $^3S_1$ contribution to $M_v{}^2$ for $^4$He. The diagrams of Fig. 2 yield

$$\langle R_{1S}(r)|j_0(\bar{\nu}r)|R_{1S}(r)\rangle\{1-\langle\Psi(^3S_1)|\Psi(^3S_1)\rangle\}$$
$$= 0.8586(-0.127) = 0.109 .$$

The complete normalization contribution is

$$\frac{\langle\Psi(^3S_1)|j_0(\bar{\nu}r)|\Psi(^3S_1)\rangle}{\langle\Psi(^3S_1)|\Psi(^3S_1)\rangle} - \langle\Psi(^3S_1)|j_0(\bar{\nu}r)|\Psi(^3S_1)\rangle$$
$$= 0.8849 - 0.9973 = -0.1124 .$$

After also investigating the effect of the diagrams in Fig. 2 on the $^1S_O$ contribution to $M_v{}^2$, we find that $M_v{}^2$ is reduced by ~27% (for $^4$He) if only the diagrams in Fig. 2 are included. As mentioned on the previous page, including the higher order diagrams (i.e., the complete normalization contribution) yields a reduction of 24% in $M_v{}^2$.

We now compare the total capture rate obtained in the closure approximation (with and without correlations) to the experimental results. Adopting the coupling constant values listed in Ref. 1 and using the recoil corrections ($\Lambda'_{\mu c}$) given by Refs. 4 and 19 we obtain for $^{16}$O ($b = 1.8$ fm, $\bar{\nu} = 0.425$ fm$^{-1}$)

$$\Lambda_{\mu c}^{\exp} = (0.98 \pm 0.05)\times 10^5 \text{ s}^{-1} \quad \text{(Ref. 20)}$$
$$= (0.97 \pm 0.03)\times 10^5 \text{ s}^{-1} \quad \text{(Ref. 21)} ,$$
$$\Lambda_{\mu c}^{\text{osc}} = 1.57\times 10^5 \text{ s}^{-1} ,$$
$$\Lambda_{\mu c}^{\text{corr}} = 1.10\times 10^5 \text{ s}^{-1} ,$$

while for $^4$He ($b = 1.38$ fm, $\bar{\nu} = 0.4$ fm$^{-1}$)

$$\Lambda_{\mu c}^{\exp} = 336 \pm 75 \text{ s}^{-1} \quad \text{(Ref. 22)}$$
$$= 375 \pm 46 \text{ s}^{-1} \quad \text{(Ref. 23)} ,$$
$$\Lambda_{\mu c}^{\text{osc}} = 375 \text{ s}^{-1} ,$$
$$\Lambda_{\mu c}^{\text{corr}} = 317 \text{ s}^{-1} .$$

The latter two results for $^4$He include corrections due to its light mass.[1]

The effect of correlations definitely improves agreement with experiment in the case of $^{16}$O and there seems to be no need to drastically alter $\bar{\nu}$ or the coupling constants $G_p$, $G_a$, and $G_v$. The results for $^4$He are now in somewhat less agreement with experiment. Again, however, the discrepancy is not serious enough to cause concern over the values of $\bar{\nu}$ or the coupling constants. We do not wish to emphasize a detailed comparison with experiment here but would simply point out that the inclusion of correlations results in a substantial reduction of the predicted total capture rate in the closure approximation.

### B. Discussion

Adopting the closure approximation and using the linked cluster expansion to introduce correlations in the target ground state wave-functions, we have calculated the muon capture matrix elements $M_v{}^2$, $M_p{}^2$, and $M_a{}^2$. The sensitivity of the results to the various approximate treatments of the Pauli operator, the energy gap between occupied and unoccupied states, and the inclusion of diagrams ensuring pair conservation has been discussed or exhibited. We find that the introduction of correlations reduces the total capture rate in $^4$He and $^{16}$O and, using those parameter values and approximations preferred, largely eliminates the experimental-theoretical discrepancy for $^{16}$O.

By varying the intermediate states excluded by the Pauli operator we found that the bulk of the reduction results from relatively low-lying 2p-2h admixtures in the g.s. These results indicate that a standard configuration-mixing shell calculation using realistic forces should also yield a reduction factor for the total capture. An earlier calculation of this type considering only pairing correlations did not yield a reduction factor.[8] Thus it would be of considerable interest to see what a more detailed shell model calculation would yield.

The major approximation in our calculations lies in replacing the exact $Q$ by $Q_{\text{AA}}$ or $Q_{\text{EE}}$ ($\mathfrak{N}$). It is hard to judge the effects of this approximation—even though it works quite well in binding energy calculations—and it would therefore be of interest to carry out linked cluster calculations in the SP representation. Of course, both this calculation and the shell model calculation suggested in the preceding paragraph are practical only because the reduction effect comes mainly from low-lying admixtures in the g.s.

*Work supported in part by the National Science Foundation.

†Present address: Physics Department, University of Arizona, Tucson, Arizona 87521.

[1]L. L. Foldy and J. D. Walecka, Nuovo Cimento 34, 1026 (1964).

[2]L. L. Foldy and J. D. Walecka, Phys. Rev. 140, B1339 (1965).

[3]H. Primakoff and C. W. Kim, Phys. Rev. 139, B1447 (1965); *ibid.* 140, B566 (1965); *ibid.* 146, 691 (1966); *ibid.* 147, 1034 (1966); *ibid.* 151, 1261 (1966).

[4]J. R. Luyten, H. P. C. Rood, and H. A. Tolhoek, Nucl. Phys. 41, 236 (1963).

[5]T. DeForest, Jr., Phys. Rev. 139, B1217 (1965).

[6]G. E. Walker, Phys. Rev. 174, 1290 (1968).

[7]A. M. Green and M. Rho, Nucl. Phys. A130, 112 (1969).

[8]G. E. Walker, Phys. Rev. C 5, 1540 (1972).

[9]A. B. Migdal, in *Many-Body Description of Nuclear Structure and Reactions, Proceedings of the International School of Physics "Enrico Fermi," Course XXXVI, 1966,* edited by C. Bloch (Academic, New York, 1966); A. B. Migdal and A. I. Larkin, Nucl. Phys. 51, 561 (1964).

[10]G. G. Bunatyan, Yad. Fiz. 2, 868 (1965) [transl.: Sov. J. Nucl. Phys. 3, 613 (1966)].

[11]G. E. Walker, Phys. Rev. 151, 745 (1966).

[12]D. J. Thouless, *The Quantum Mechanics of Many-Body Systems* (Academic, New York, 1961); B. H. Brandow, Rev. Mod. Phys. 39, 771 (1967).

[13]R. J. McCarthy and G. E. Walker, Phys. Rev. C 9, 809 (1974); R. J. McCarthy, Phys. Lett. (to be published).

[14]R. L. Becker, A. D. MacKellar, and B. M. Morris, Phys. Rev. 174, 1264 (1968); K. T. R. Davies and R. J. McCarthy, Phys. Rev. C 4, 81 (1971).

[15]B. R. Barrett, R. G. L. Hewitt, and R. J. McCarthy, Nucl. Phys. A184, 13 (1972).

[16]R. J. Eden and V. J. Emery, Proc. R. Soc. Lond. A248, 288 (1958).

[17]C. W. Wong, Nucl. Phys. A91, 399 (1967).

[18]B. R. Barrett, R. G. L. Hewitt, and R. J. McCarthy, Phys. Rev. C 3, 1137 (1971).

[19]L. J. Tassie and F. C. Barker, Phys. Rev. 111, 940 (1958).

[20]J. Barlow, J. C. Sens, P. J. Duke, and M. A. R. Kemp, Phys. Lett. 9, 84 (1964).

[21]M. Eckhouse, Ph.D. thesis, Carnegie Institute of Technology, Pittsburgh, 1962 (unpublished) (NYO-9286).

[22]R. Bizzarri, E. D. Capua, V. Dore, G. Gislanella, P. Guidoni, and I. Laakso, Nuovo Cimento 33, 1497 (1964).

[23]M. Bloch, quoted as private communication in Ref. 1.